

## Fe<sub>3</sub>O<sub>4</sub> Decorated Reduced Graphene Oxide Modified Electrode for Electrochemistry of Hemoglobin and Its Application as Trichloroacetic acid and Nitrite Sensor

Hui Xie<sup>1,2</sup>, Juan Liu<sup>3</sup>, Hamza Abdalla Yones<sup>2</sup>, Yanyan Niu<sup>1</sup>, Yixing Zhao<sup>1</sup>, Yaru Xi<sup>2</sup>, Xiaobao Li<sup>2</sup>, Guangjiu Li<sup>3</sup>, Wei Sun<sup>2,\*</sup>, Xianghui Wang<sup>1,\*</sup>

<sup>1</sup> Key Laboratory of Water Pollution Treatment and Resource Reuse of Hainan Province, Hainan Normal University, Haikou 571158, China

<sup>2</sup> Key Laboratory of Laser Technology and Optoelectronic Functional Materials of Hainan Province, College of Chemistry and Chemical Engineering, Hainan Normal University, Haikou 571158, China

<sup>3</sup> Key Laboratory of Optic-electric Sensing and Analytical Chemistry for Life Science of Ministry of Education, Qingdao University of Science and Technology, Qingdao 266042, China

\*E-mail: [swyy26@hotmail.com](mailto:swyy26@hotmail.com) and [god820403@163.com](mailto:god820403@163.com)

Received: 5 June 2019 / Accepted: 12 July 2019 / Published: 5 August 2019

---

An electrochemical biosensor was designed by using Fe<sub>3</sub>O<sub>4</sub>@reduced graphene oxide (Fe<sub>3</sub>O<sub>4</sub>@rGO) composite as the electrode modifier. Hemoglobin (Hb) could achieve direct electron transfer on the modified electrode due to the advantages of Fe<sub>3</sub>O<sub>4</sub>@rGO such as remarkable conductivity, excellent biocompatibility and big surface area. In addition, this electrochemical biosensor (Nafion/Hb/Fe<sub>3</sub>O<sub>4</sub>@rGO/CILE) also displayed electrocatalytic performance to different substrates such as trichloroacetic acid (TCA) and sodium nitrite (NaNO<sub>2</sub>) with the detection limit as 1.67 mmol/L and 13.33 μmol/L (3σ). The apparent Michaelis-Menten constant ( $K_M^{app}$ ) were calculated as 33.89 mmol/L and 0.44 mmol/L, respectively. Furthermore, real samples (medical facial peel solution and pickle juice solution) were analyzed by this electrochemical sensor with acceptable recoveries. Therefore, Fe<sub>3</sub>O<sub>4</sub>@rGO modified electrode was used for the construction of electrochemical sensing device with the ability to accelerate the electron communication of Hb.

---

**Keywords:** Fe<sub>3</sub>O<sub>4</sub>@reduced graphene oxide; Hemoglobin; Direct electron transfer; Electrocatalysis; Electrochemical biosensor

### 1. INTRODUCTION

Direct electron transfer (DET) between redox protein/enzyme and electrode is of very significance in the fields of bioelectrochemistry and biosensor. The mechanism of DET and electrocatalytic reactions can give lots of information to understand the process of biological redox

reaction [1, 2]. As one of typical redox protein, hemoglobin (Hb) is responsible for the transport of oxygen in red blood cells. However, the electroactive centers of ferroporphyrins are wrapped by polypeptide chains, which is hardly to transfer electrons. Therefore different modifiers and films have been used to solve this problem with the DET process realized [3, 4].

Various nanomaterials such as metallic oxides, transitional metal dichalcogenides, graphene (GR) and its derivatives have been selected for the fabrication of sensors [5]. Among them, GR has been especially considered as a “rising star” with different applications in electrochemical energy storage, biosensors and electronics due to its specific mechanical, electrical and chemical properties [6, 7]. However, the use of pristine GR has proved challenging on account of difficult bottom-up synthesis, poor solubility, and easy agglomeration in solution due to Vander Waals interactions [8]. As the precursor of GR, graphene oxide (GO) can be used for the synthesis of the nanocomposite, which can act as the carrier for the loading of other nanomaterials with abundant oxygen-based functional groups [9]. In order to recovery the electrochemical properties, GO can be treated by a number of methods to get reduced graphene oxide (rGO), which can minimize the content of oxygenal groups and achieve properties closer to those of pristine GR [10]. Therefore, GR and its related composite have been used as potential electrode materials due to the flexibility, chemical structure, electrical conductivity and large surface area [11]. For example, Deng’s group applied GR and functionalized GR for the electrochemical detection of various electroactive substances [12-16]. Our group fabricated metal or metal oxide decorated GR modified electrode for electrochemical biosensing applications [17-20].

Fe<sub>3</sub>O<sub>4</sub> nanoparticle is a commonly used nanomaterial that exhibits widely physicochemical applications due to the outstanding electrochemical properties, cheap operational potential, low cost and environmental friendliness, which can be used as the sensitizer to increase the performances of transduction platform [21]. In this paper, Fe<sub>3</sub>O<sub>4</sub> decorated rGO nanocomposite (Fe<sub>3</sub>O<sub>4</sub>@rGO) was chosen as the modifier for the design of chemical modified interface, which was further used to achieve the DET of Hb. Electrochemistry and electrocatalysis of Hb was accelerated on this Fe<sub>3</sub>O<sub>4</sub>@rGO modified electrode.

## 2. EXPERIMENTAL

### 2.1 Chemicals

N-Hexylpyridinium hexafluorophosphate (HPPF<sub>6</sub>, Lanzhou Yulu Fine Chem. Co., China), graphite powder (Shanghai Colloid Chem. Co., China), Fe<sub>3</sub>O<sub>4</sub>@reduced graphene oxide (Fe<sub>3</sub>O<sub>4</sub>@rGO, Nanjing XFNANO Co., China), Hb (Sigma, USA) and 5.0% Nafion (Dupont, USA) were used as received. The supporting electrolyte for the electrochemical studies was 0.1 mol/L phosphate buffer solution (PBS) and ultrapure water (Milli-Q, USA) was used in the experiment.

### 2.2 Instruments

Electrochemical tests were conducted on a CHI 660D electrochemical analyzer (Shanghai CH Instrument, China). Three-electrode system was consisted of the modified electrode as working

electrode, platinum electrode as counter electrode and saturated calomel electrode (SCE) as reference electrode. The morphology of  $\text{Fe}_3\text{O}_4@\text{rGO}$  was investigated by JSM-7100F scanning electron microscopy (SEM, JEOL, Japan).

### 2.3 Fabrication of Nafion/Hb/ $\text{Fe}_3\text{O}_4@\text{rGO}/\text{CILE}$

CILE was prepared by previous work [22]. 0.5 mg/mL  $\text{Fe}_3\text{O}_4@\text{rGO}$  dispersion was prepared in ultrapure water by 3 hours ultrasonication, which was further covered on CILE surface with the volume of 8.0  $\mu\text{L}$  and dried at natural conditions. Then, 8.0  $\mu\text{L}$  15.0 mg/mL Hb solution and 6.0  $\mu\text{L}$  0.5% Nafion solution were pipetted in sequence and dried naturally to obtain the working electrode (Nafion/Hb/ $\text{Fe}_3\text{O}_4@\text{rGO}/\text{CILE}$ ).

### 2.4 Procedure

Electrochemical impedance spectroscopy (EIS) were recorded in a 10.0 mmol/L  $\text{K}_3[\text{Fe}(\text{CN})_6]$  and 0.1 mol/L KCl mixture with the frequency from  $10^5$  to  $10^{-1}$  Hz. Cyclic voltammetric (CV) experiments were performed in a  $\text{N}_2$ -saturated 0.10 mol/L pH 3.0 PBS with scan rate of 100 mV/s. The determinations of TCA or  $\text{NaNO}_2$  content in real samples were operated with the following steps. Medical facial peel solution or pickle juice solution were diluted by pH 3.0 PBS and analyzed based on the above procedure. Then standard solutions were added in the sample solution to evaluate the recoveries.

## 3. RESULTS AND DISCUSSION

### 3.1 SEM of $\text{Fe}_3\text{O}_4@\text{rGO}$

The morphology and structure of  $\text{Fe}_3\text{O}_4@\text{rGO}$  were observed by SEM with the data presented in Fig. 1. It can be observed that  $\text{Fe}_3\text{O}_4$  nanoparticles were uniformly distributed on rGO surface, and rGO exhibited with a 3D pleated and porous structure that formed by stacked multilayer rGO sheets.

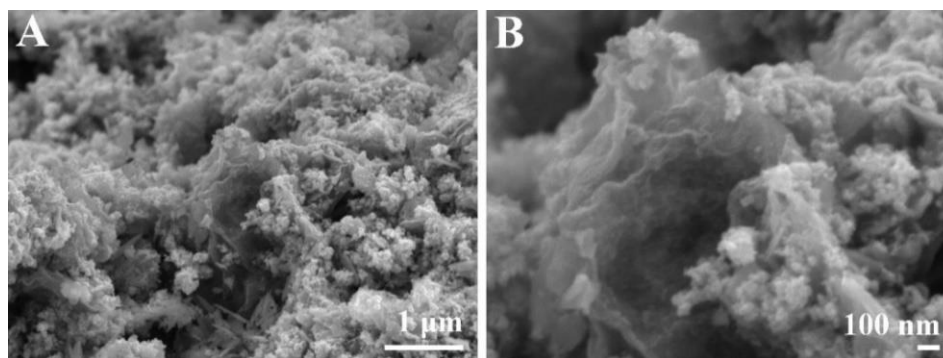


**Figure 1.** SEM of  $\text{Fe}_3\text{O}_4@\text{rGO}$  at different magnification.

### 3.2 Electrochemical investigations

EIS was conducted with the curves shown in Fig. 2A and the electron transfer resistance ( $R_{et}$ ) values of different modified electrodes were measured. On  $Fe_3O_4@rGO/CILE$  (curve a) a straight line was recorded, indicating the good conductivity of  $Fe_3O_4@rGO$  composite with the oxygen-containing functional groups decreased after GO reduced. Nafion/CILE (curve d) and Nafion/Hb/CILE (curve e) gave the  $R_{et}$  values of 178  $\Omega$  and 230  $\Omega$ , which were larger than that of CILE (curve c, 137  $\Omega$ ). The results were due to the non-conductive Hb and Nafion severely impeded the interfacial electron transfer. While on Nafion/Hb/ $Fe_3O_4@rGO/CILE$  (curve b) the  $R_{et}$  value of 42  $\Omega$  demonstrated that the presence of  $Fe_3O_4@rGO$  was beneficial for electron transduction.

Excellent conductivity and large specific surface area of  $Fe_3O_4@rGO$  composite can provide remarkable interface for Hb to achieve direct electrochemistry. Hence, electrochemical behaviors of different modified electrodes were recorded by CV with curves shown in Fig. 2B. Neither Nafion/CILE (curve d) nor Nafion/ $Fe_3O_4@rGO/CILE$  (curve c) displayed redox peaks, revealing no electroactive substances existed on the modified electrodes. In addition, the background current of Nafion/CILE was smaller than Nafion/ $Fe_3O_4@rGO/CILE$ , which was ascribed to the presence of  $Fe_3O_4@rGO$  composite that expanded the effective surface area of electrode. A pair of redox peaks with poor reversibility was observed on Nafion/Hb/CILE, which meant that the redox reaction of Hb heme was realized on electrode with a slow electron transfer. However on Nafion/Hb/ $Fe_3O_4@rGO/CILE$  (curve a) a distinctly current response with a pair of well-defined redox peak appeared. The reduction peak potential ( $E_{pc}$ ) at -0.234 V and the oxidation peak potential ( $E_{pa}$ ) at -0.166 V were got with the separation of peak potential ( $\Delta E_p$ ) of -0.068 V and the  $I_{pa}/I_{pc}$  close to 1, proving that the excellent conductivity of  $Fe_3O_4@rGO$  established a path for electron transfer between electrode and electroactive center of Hb. Moreover, the large specific surface area of  $Fe_3O_4@rGO$  was beneficial for the loading of more Hb with effective signal amplification. Therefore, DET of Hb was accelerated with the modification of  $Fe_3O_4@rGO$  nanocomposite on the electrode surface.

The effect of scan rate towards the voltammetric behavior of Hb was checked by CV with the data present in Fig. 2C. The peak current varied linearly with scan rate from 10 to 800 mV/s and this dependence to the logarithmic scale was almost to unity, proving this process was surface-controlled [23]. The integration of the redox peak resulted in nearly constant charge with scan rate, which was a characteristic of thin layer electrochemical behavior [24]. The average surface concentration ( $\Gamma$ ) of electroactive Hb present on Nafion/Hb/ $Fe_3O_4@rGO/CILE$  was got from the slope of  $I_p$  versus scan rate [25] with  $\Gamma_{Hb}$  calculated as  $5.06 \times 10^{-9}$  mol/cm<sup>2</sup>, which was bigger than the theoretical value for a monolayer coverage ( $1.89 \times 10^{-11}$  mol/cm<sup>2</sup>) [26]. Bu using Laviron's equation [27], the heterogeneous electron transfer rate constant ( $k_s$ ) was calculated as 1.30 s<sup>-1</sup>, indicating that the presence of  $Fe_3O_4@rGO$  promoted DET of Hb heme to the electrode.

CV curves of Nafion/Hb/ $Fe_3O_4@rGO/CILE$  in different pH PBS were recorded with the data present in Fig. 2D. A pair of redox peaks was observed at each pH, indicating Hb retained electroactive under different microenvironment. The peak potential was slowly moved and the formal potential ( $E^{0'}$ ) shifted negatively with pH, indicating that the redox reaction of Hb heme Fe(III)/Fe(II) involved proton transfer. A linear relationship between  $E^{0'}$  and pH was got within the range of 3.0 to

9.0 and the regression equation was  $E^{0'} (\text{V}) = -0.060 \text{ pH} - 0.15$  ( $\gamma = 0.983$ ). The obtained slope value (-60 mV/pH) was same as the theoretical value (-59 mV/pH) of the Nernst equation for a reversible electrode process with equal number of electrons and protons [28]. Moreover, the highest current signal was got at pH 3.0, which was selected for investigation on the redox reaction of Hb.

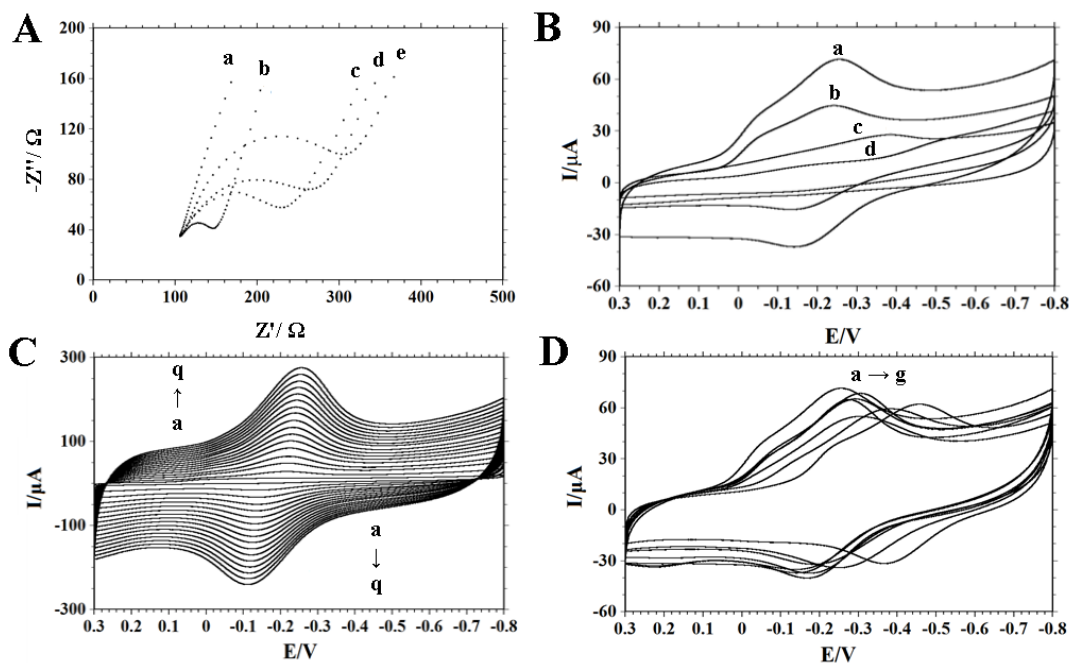


**Figure 2.** (A) EIS of  $\text{Fe}_3\text{O}_4@\text{rGO}/\text{CILE}$  (a),  $\text{Nafion}/\text{Hb}/\text{Fe}_3\text{O}_4@\text{rGO}/\text{CILE}$  (b),  $\text{CILE}$  (c),  $\text{Nafion}/\text{CILE}$  (d) and  $\text{Nafion}/\text{Hb}/\text{CILE}$  (e) with frequency from  $10^5$  to 0.1 Hz in a 10.0 mmol/L  $[\text{Fe}(\text{CN})_6]^{3-/4-}$  and 0.1 mol/L KCl mixture solution; (B) CV curves of  $\text{Nafion}/\text{Hb}/\text{Fe}_3\text{O}_4@\text{rGO}/\text{CILE}$  (a),  $\text{Nafion}/\text{Hb}/\text{CILE}$  (b),  $\text{Nafion}/\text{Fe}_3\text{O}_4@\text{rGO}/\text{CILE}$  (c) and  $\text{Nafion}/\text{CILE}$  (d) in pH 3.0 PBS with the scan rate of 100 mV/s; (C) Influence of scan rate on voltammetric behavior of  $\text{Nafion}/\text{Hb}/\text{Fe}_3\text{O}_4@\text{rGO}/\text{CILE}$  in pH 3.0 PBS (from a to q as 10, 50, 100, 150, 200, 250, 300, 350, 400, 450, 500, 550, 600, 650, 700, 750, 800 mV/s); (D) Effect of pH on voltammetric behavior of  $\text{Nafion}/\text{Hb}/\text{Fe}_3\text{O}_4@\text{rGO}/\text{CILE}$  at scan rate of 100 mV/s (from a to g 3.0, 4.0, 5.0, 6.0, 7.0, 8.0, 9.0).

### 3.3 Electrocatalytic performances

After successfully achieving DET of Hb at  $\text{Fe}_3\text{O}_4@\text{rGO}$  modified electrode, electrocatalytic performance towards different substrates were explored. Due to similar active center of Hb with enzymes containing the heme group,  $\text{Nafion}/\text{Hb}/\text{Fe}_3\text{O}_4@\text{rGO}/\text{CILE}$  was used to discuss the mechanism of enzyme-substrate interaction. As shown in Fig 3, electrocatalytic activity of TCA was investigated and the addition of TCA led to two reduction peaks at -0.283 V and -0.547 V with current increased gradually. While the oxidation peak current decreased and disappeared finally. This catalytic behavior was a typical process of the stepwise reduction of TCA to dichloroacetic acid, chloroacetic acid and acetic acid [29]. Electrocatalytic current ( $I_{pc}$ ) had a linear relationship with TCA concentration in the range of 5.0 mmol/L to 310.0 mol/L with the regression equation as  $I_{pc} (\mu\text{A}) =$

2.68 C (mmol/L) + 158.04 ( $\gamma = 0.992$ ) and the detection limit as 1.67 mmol/L ( $3\sigma$ ). With the increase of TCA concentration, a characteristic plateau of Michaelis-Menten behavior appeared. Based on the following Lineweaver-Burk equation [30]:  $\frac{1}{I_{ss}} = \frac{1}{I_{max}} + \frac{K_M^{app}}{I_{max}} \cdot \frac{1}{C}$ , the apparent Michaelis-Menten constant ( $K_M^{app}$ ) was calculated as 33.89 mmol/L.

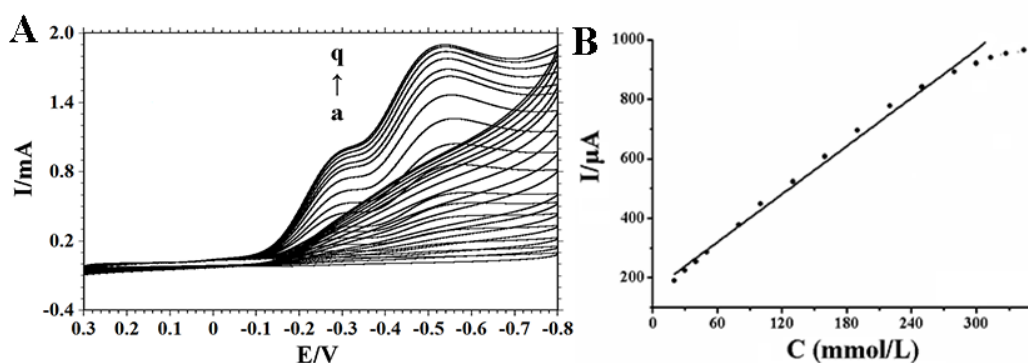


**Figure 3.** (A) CV curves of Nafion/Hb/Fe<sub>3</sub>O<sub>4</sub>@rGO/CILE with different TCA concentration (from a to q as 0, 10, 20, 30, 40, 50, 60, 70, 80, 100, 130, 160, 190, 220, 250, 280, 310 mmol/L) in pH 3.0 PBS at the scan rate of 100 mV/s; (B) The linear relationship between  $I_{pc}$  and the TCA concentration.

Redox enzyme also has the capacity to bind with nitrite, therefore NaNO<sub>2</sub> was catalyzed by Nafion/Hb/Fe<sub>3</sub>O<sub>4</sub>@rGO/CILE. Fig. 4 depicted the reduction process of NaNO<sub>2</sub> with the reduction peak of NO<sub>2</sub><sup>-</sup> at -0.617 V. In the NaNO<sub>2</sub> concentration range from 0.04 mmol/L to 1.80 mmol/L, the linear regression equation was obtained as  $I_{pc}(\mu A) = 88.61 C \text{ (mmol/L)} + 24.91$  ( $\gamma = 0.992$ ) with the detection limit of 13.33  $\mu\text{mol/L}$  ( $3\sigma$ ). While the NaNO<sub>2</sub> concentration exceeded 1.80 mmol/L,  $I_{pc}$  became steady with the  $K_M^{app}$  calculated as 0.44 mmol/L. As a comparison, the analytical parameters for TCA or nitrite detection using different biosensors were summarized in Table 1, which indicated that this modified electrode had relatively wide linear range and low detection limit.

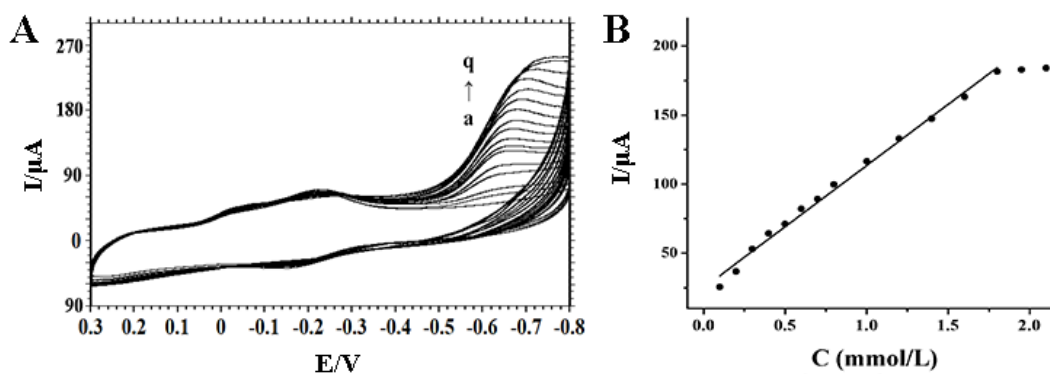


**Figure 4.** (A) CV curves of Nafion/Hb/Fe<sub>3</sub>O<sub>4</sub>@rGO/CILE with different NaNO<sub>2</sub> concentration (from a to q as 0, 0.04, 0.06, 0.14, 0.20, 0.26, 0.32, 0.38, 0.45, 0.55, 0.65, 0.75, 0.95, 1.10, 1.40, 1.60, 1.80 mmol/L) in pH 3.0 PBS at the scan rate of 100 mV/s; (B) The linear relationship between  $I_{pc}$  and the NaNO<sub>2</sub> concentration.

**Table 1.** Comparison of analytical parameters of TCA or nitrite detection by different biosensors.

Biosensors	Analyte	Linear range (mmol/L)	Detection limit (mmol/L)	$K_M^{app}$ (mmol/L)	Ref.
Nafion/HRP/Co <sub>3</sub> O <sub>4</sub> /CILE	TCA	5.00–90.00	1.70	88.15	[31]
Nafion/Mb/TiO <sub>2</sub> @CNF/CILE	TCA	5.00–105.00	1.60	5.06	[32]
Mb/DNA/CILE	TCA	0.50–40.00	83.00	0.82	[33]
BP-PEDOT:PSS-Hb/CILE.	TCA	3.00–460.00	1.00	14.30	[34]
Hb-meso-Al <sub>2</sub> O <sub>3</sub> -PVA/GCE	nitrite	0.20–10.00	0.03	/	[35]
Nafion/Hb/TNTs/CILE	nitrite	0.30–17.00	0.083	2.74	[36]
Nafion/Mb/SWCNTs/GCE	nitrite	0.50–5.00	0.95	6.45	[37]
CTS-Hb-CNT-IL/CILE	nitrite	0.40–8.00	0.10	0.10	[38]
Nafion/Hb/Fe <sub>3</sub> O <sub>4</sub> @rGO/CILE	TCA	5.00–310.00	1.67	33.89	This work
	nitrite	0.04–1.80	0.013	0.44	

### 3.4 Samples analysis

TCA content in medical facial peel solution or NaNO<sub>2</sub> content in pickle juice solution were analyzed using Nafion/Hb/Fe<sub>3</sub>O<sub>4</sub>@rGO/CILE by standard curve method with the results displayed in Table 2. The recoveries were obtained by standard addition method with the values got as 92.20% to 96.63% and 90.00% to 95.00%, respectively, demonstrating a practical usage of the proposed method for TCA and NaNO<sub>2</sub> analysis in real samples.

**Table 2.** Content analysis of TCA or NaNO<sub>2</sub> in real samples by Nafion/Hb/Fe<sub>3</sub>O<sub>4</sub>@rGO/CILE (n = 3).

Samples	Marked (mmol/L)	Detected (mmol/L)	Added (mmol/L)	Total (mmol/L)	Recovery (%)
Medical facial peel solution	57.67	57.82	10.00	67.04	92.20
			20.00	76.70	94.40
			30.00	86.81	96.63
Pickle juice solution	/	1.14	0.10	1.23	90.00
			0.20	1.33	95.00
			0.30	1.42	93.33

#### 4. CONCLUSION

In this paper Fe<sub>3</sub>O<sub>4</sub>@rGO nanocomposite was acted as the electrode sensitizer to fabricate a redox protein based electrochemical biosensor. Fe<sub>3</sub>O<sub>4</sub>@rGO displayed excellent conductivity, bigger specific surface area and outstanding biocompatibility, which could form an efficient transduction platform for Hb to achieve DET. Moreover, the immobilized Hb exhibited excellent electrocatalytic behavior toward different substances including TCA and NaNO<sub>2</sub> with wide analytical range, low detection limit and fast current response, which proved the potential applications of Fe<sub>3</sub>O<sub>4</sub>@rGO nanocomposite in nanointerface-based electrochemical biosensing fields.

#### ACKNOWLEDGEMENTS

This project was supported by the Natural Science Foundation of Hainan Province of China (2017CXTD007), the Key Science and Technology Program of Haikou City (2017042), Research Fund from Beijing Innovation Center for Future Chips (KYJJ2018006), Project of University Student Entrepreneurship Training Program of Hainan Province (30101100331), the Key Research and Development Program of Hainan Province - Social Development Direction (ZDYF2018170).

#### References

1. F. Armstrong, H.A. O Hill and N.J. Walton, *Acc. Chem. Res.*, 21 (1988) 407.
2. X.L. Niu, H. Xie, G.L. Luo, Y.L. Men, W.L. Zhang and W. Sun, *J. Electrochem. Soc.*, 165 (2018) B713.
3. A. Heller, *Acc. Chem. Res.*, 23 (1991) 67.
4. W. Chen, W.J. Weng, X.L. Niu, X.Y. Li, Y.L. Men, W. Sun, G.J. Li and L.F. Dong, *J. Electroanal. Chem.*, 823 (2018) 137.
5. W. Chen, W.J. Weng, C.X. Yin, X.L. Niu, G.J. Li, H. Xie, J. Liu and W. Sun, *Int. J. Electrochem. Sci.*, 13 (2018) 4741.
6. M.L. Yola, V.K. Gupta, T. Eren, A.E. Şen and N. Atar, *Electrochim. Acta*, 120 (2014) 204.
7. M.L. Yola, N. Atar, Z. Üstündağ, and A.O. Solak, *J. Electrochem. Soc.*, 698 (2013) 9.
8. T. Kuilla, S. Bhadra, D. Yao, N.H. Kim, S. Bose and J.H. Lee, *Prog. Polym. Sci.*, 35 (2010) 1350.
9. A.T. Smith, A.M. LaChance, S.S. Zeng, B. Li and L.Y. Sun, *Nano Materials Science*, 1 (2019) 31.
10. S.F. Pei and H.M. Cheng, *Carbon*, 50 (2012) 3210.
11. N. Atar, T. Eren and M.L. Yola, *Thin Solid Films*, 590 (2015) 156.
12. K.Q. Deng, J.H. Zhou and X.F. Li, *Electrochim. Acta*, 95 (2013) 18.
13. K.Q. Deng, J.H. Zhou and X.F. Li, *Electrochim. Acta*, 114 (2013) 341.
14. K.Q. Deng, J.H. Zhou, H.W. Huang, Y.L. Ling and C.X. Li, *Anal. Lett.*, 49 (2016) 2917.
15. K.Q. Deng, C.X. Li, X.Y. Qiu, J.H. Zhou and Z.H. Hou, *J. Electroanal. Chem.*, 755 (2015) 197.
16. K.Q. Deng, C.X. Li, X.F. Li and H.W. Huang, *J. Electroanal. Chem.*, 780 (2016) 296.
17. X.L. Niu, Z.R. Wen, X.B. Li, W.S. Zhao, X.Y. Li, Y.Q. Huang, Q.T. Li, G.J. Li and W. Sun, *Sensor. Actuat. B-Chem.*, 255 (2018) 471.
18. X.B. Li, X.L. Niu, W. Chen, L.F. Dong, Y.Y. Niu, T.M. Shao, W.T. Lai and W. Sun, *Int. J. Electrochem. Sci.*, 12 (2017) 9774.
19. Z.R. Wen, W.S. Zhao, X.Y. Li, X.L. Niu, X.L. Wang, L.J. Yan, X. Zhang, G.J. Li and W. Sun, *Int. J. Electrochem. Sci.*, 12 (2017) 2306.
20. X. L. Niu, X. Y. Li, W. Chen, X. B. Li, W. J. Weng, C. X. Yin, R. X. Dong, W. Sun and G. J. Li, *Mat. Sci. Eng. C.*, 89 (2018) 230.
21. G. Venkataprasad, T.M. Reddy, A.L. Narayana, O.M. Hussain, P. Shaikshavali, T.V. Gopal and P.

- Gopal, *Sens. Actuators, A*, 93 (2019) 87.
22. W.J. Weng, J. Liu, C.X. Yin, H. Xie, G.L. Luo, W. Sun, G.J. Li, *Int. J. Electrochem. Sci.*, 14 (2019) 4309.
23. W. Chen, X.L. Niu, X.Y. Li, X.B. Li, G.J. Li, B.L. He, Q.T. Li and W. Sun, *Mater. Sci. Eng. C*, 80 (2017) 135.
24. W. Zheng, W.S. Zhao, W. Chen, W.J. Weng, Z.W. Liao, R.X. Dong, G.J. Li and W. Sun, *Int. J. Electrochem. Sci.*, 12 (2017) 4341.
25. E. Laviron, *J. Electroanal. Chem.*, 100 (1979) 263.
26. S.F. Wang, T. Chen, Z.L. Zhang, X.C. Shen, Z.X. Lu, D.W. Pang and K.Y. Wong, *Langmuir*, 21 (2005) 9260.
27. E. Laviron, *J. Electroanal. Chem.*, 101 (1979) 19.
28. A.J. Bard and L.R. Faulkner, *Electrochemical Methods: Fundamentals and Applications*, Wiley, New York, 1980.
29. Y.Y. Niu, H. Xie, G.L. Luo, W.J. Weng, C.X. Ruan, G.J. Li and W. Sun, *RSC Adv.*, 9 (2019) 4480.
30. R.A. Kamin and G.S. Wilson, *Anal. Chem.*, 52 (1980) 1198.
31. W. Chen, W.J. Weng, C.X. Yin, X.L. Niu, G.J. Li, H. Xie, J. Liu and W. Sun, *Int. J. Electrochem. Sci.*, 13 (2018) 4741.
32. Y.Y. Niu, H. Xie, G.L. Luo, W.J. Weng, C.X. Ruan, G.J. Li and W. Sun, *RSC Adv.*, 9 (2019) 4480.
33. R. F. Gao and J. B. Zheng, *Electrochem. Commun.*, 11 (2009) 1527.
34. X.Y. Li, X.L. Niu, W.S. Zhao, W. Chen, C.X. Yin, Y.L. Men, G.J. Li and W. Sun, *Electrochem. Commun.*, 86 (2018) 68.
35. J.J. Yu, J.R. Ma, F.Q. Zhao and B.Z. Zeng, *Electrochim. Acta* 53 (2008) 1995.
36. W.J. Weng, J. Liu, C.X. Yin, H. Xie, G.L. Luo, W. Sun and G.J. Li, *Int. J. Electrochem. Sci.*, 14 (2019) 4309.
37. G.L. Turdean and G. Szabo. *Food Chem.*, 179 (2015) 325.
38. Z.H. Zhu, L.N. Qu, X. Li, Y. Zeng, W. Sun and X.T. Huang, *Electrochim. Acta* 55 (2010) 5959.